Science of the Total Environment 750 (2021) 141592

Contents lists available at ScienceDirect

Science of the Total Environment

journal homepage: www.elsevier.com/locate/scitotenv

Spatiotemporal impacts of COVID-19 on air pollution in California, USA

Qian Liu [a,b], Jackson T. Harris [a,c], Long S. Chiu [d], Donglian Sun [b], Paul R. Houser [b], Manzhu Yu [e], Daniel Q. Duffy [f], Michael M. Little [f], Chaowei Yang [a,b,*]

[a] NSF Spatiotemporal Innovation Center, George Mason Univ., Fairfax, VA 22030, USA
[b] Department of Geography and GeoInformation Science, George Mason Univ., Fairfax, VA 22030, USA
[c] Department of Geography, Dartmouth College, Hanover, NH 03755, USA
[d] Department of Atmospheric, Oceanic and Earth Sciences, George Mason Univ., Fairfax, VA 22030, USA
[e] Department of Geography, Pennsylvania State University, State College, PA 16801, USA
[f] NASA Goddard, Computational and Information Sciences and Technology Office, Greenbelt, MD 20771, USA

HIGHLIGHTS

- The impacts of COVID-19-related interventional policies on air pollution are spatiotemporally analyzed over California.
- The lockdown policy reduced the overall emissions of air pollutants in California.
- During the lockdown, NO_2 decreased near major power plants and increased over major transportation hubs.
- After reopening, state-mean air pollution metrics returned to normal trends in California.

GRAPHICAL ABSTRACT

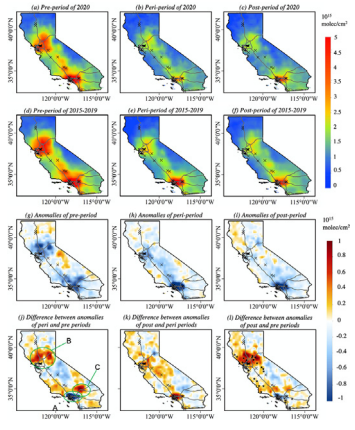

ARTICLE INFO

Article history:
Received 10 July 2020
Received in revised form 3 August 2020
Accepted 8 August 2020
Available online 10 August 2020

Editor: Jay Gan

Keywords:
COVID-19
California
Air pollution
Lockdown
Reopening

ABSTRACT

Various recent studies have shown that societal efforts to mitigate (e.g. "lockdown") the outbreak of the 2019 coronavirus disease (COVID-19) caused non-negligible impacts on the environment, especially air quality. To examine if interventional policies due to COVID-19 have had a similar impact in the US state of California, this paper investigates the spatiotemporal patterns and changes in air pollution before, during and after the lockdown of the state, comparing the air quality measurements in 2020 with historical averages from 2015 to 2019. Through time series analysis, a sudden drop and uptick of air pollution are found around the dates when shutdown and reopening were ordered, respectively. The spatial patterns of nitrogen dioxide (NO_2) tropospheric vertical column density (TVCD) show a decreasing trend over the locations of major powerplants and an increasing trend over residential areas near interactions of national highways. Ground-based observations around California show a 38%, 49%, and 31% drop in the concentration of NO_2, carbon monoxide (CO) and particulate matter 2.5 ($PM_{2.5}$) during the lockdown (March 19–May 7) compared to before (January 26–March 18) in 2020. These are 16%, 25% and 19% sharper than the means of the previous five years in the same periods, respectively. Our study offers evidence of the environmental impact introduced by COVID-19, and insight into related economic influences.

* Corresponding author at: NSF Spatiotemporal Innovation Center, George Mason University, 4400 University Dr., Exploratory Hall, Room 2211, Fairfax, VA 22030, USA.
E-mail address: cyang3@gmu.edu (C. Yang).

https://doi.org/10.1016/j.scitotenv.2020.141592
0048-9697/

1. Introduction

The unexpected outbreak of the 2019 coronavirus disease (COVID-19) has greatly impacted both economies and environments (Liu et al., 2020a, 2020b; Yang et al., 2020; Saadat et al., 2020) due to societal efforts and policies to mitigate or "lockdown" the disease by local and national governments—including the shutting-down of non-essential industries and the restriction of public transportation. Currently, the spread of coronavirus has been initially controlled in many regions of the world and some countries have chosen to reopen. Thus, evaluations of the impacts of COVID-19 on the environment and economy as well as study into infection and death rates are increasingly urgent and necessary to inform decision makers at all levels.

Air pollutants such as nitrogen dioxide (NO_2), carbon monoxide (CO), ozone (O_3) and particulate matter ($PM_{2.5}$ and PM_{10}) are important indicators of economic and human activities. For example, NO_2 is primarily emitted from fossil fuel consumption (Russell et al., 2012); and vehicle emissions are one of the primary sources of $PM_{2.5}$ (Manousakas et al., 2017). Analysis of the spatiotemporal patterns, trends and changes of air pollution can reflect the impact of COVID-19 mitigation efforts on industrial production, transportation, and changes to a population's daily activities. These metrics are essential for decision-makers to assess economic losses to inform policy implementation, and accordingly make plans for business reopening and industry resumption (Hilboll et al., 2017; Sinha, 2016). The lockdown situation offers an unprecedented opportunity to study and monitor the emissions of air pollutants from specific industrial power plants and transportation facilities. Furthermore, long-term exposure to higher concentration of $PM_{2.5}$ is proven to be associated with higher COVID-19 mortality rates (Wu et al., 2020); and $PM_{2.5}$, PM_{10}, NO_2 and O_3 were observed to have significantly positive associations with newly COVID-19 confirmed cases (Zhu et al., 2020). Therefore, understanding air pollution trends is also critical to implement a pragmatic economic reopening.

Since the start of the worldwide COVID-19 pandemic, air pollution has been observed to decline in some regions of the world through comparison of conditions before and during the COVID-19 crisis (Liu et al., 2020a, 2020b; Zhang et al., 2020; Dutheil et al., 2020; Wang et al., 2020). Still, whether reductions are due to the pandemic cannot be confirmed without a comprehensive comparison to long-term historical data in the same annual period; seasonal cycles and climate patterns are also potential causes of air pollution changes (Wang et al., 2006). Furthermore, local policies may vary significantly across different states or provinces even within the same country especially for nations like the US (Raifman et al., 2020). State governments have therefore implemented their own COVID-19 mitigation policies and administrative measures regarding to the shutdown and reopening. Existing studies of air pollution patterns for some jurisdictional regions or administrative scales may have limited referential significance for other areas. Most prior studies have focused on the areas where COVID-19 emerged first, such as China (Bao and Zhang, 2020; Wang et al., 2020) and across Europe (Muhammad et al., 2020). Liu et al. (2020a) discovered an uptick in air pollution when China began gradual reopening. Whether similar characteristics can be found in the US is still up in the air. Finally, an overall decreasing trend doesn't indicate that air pollution drops ubiquitously. It is essential to confirm and summarize specific patterns in different administrative zones for the assessment of regional economies.

This study conducts a thorough spatiotemporal analysis (Yang et al., 2019, 2020b) on the changes of air pollutants before (Jan 26–March 18), during (March 19–May 8) and after (May 9–June 14, hereafter referred to as pre, *peri* and post periods) the lockdown of California (CA), USA, in 2020, and compares the patterns with the annual means of 2015–2019 (hereafter referred to as 2015–2019) to isolate the effect of COVID-19 mitigation efforts. The locations of major power plants, wildfires and national highways are also utilized as analytical factors to explain the significance of detected patterns.

The remainder of this paper is organized as follows: the study area, datasets and analysis methods are introduced in Section 2; the results are described in Section 3; further discussion is offered in Section 4; and conclusions are given in Section 5.

2. Material and methods

2.1. Study area

This study focuses on the state of California, where more than 150,000 cases were reported by June 14—the second-highest number among all US states—and more than 5000 deaths were directly attributable to the virus (NSF STC, 2020). Fig. 1 shows the cumulative confirmed cases numbers of each county in CA by June 14. Government response to the situation steadily grew more severe as case numbers increased. As the death toll increased around the state, California Governor declared a state of emergency and gradually increased lockdown orders, beginning on March 4. By March 19, the state shutdown all the non-essential business and a statewide lockdown order was issued. On May 8, fifty days later, a 4-phase reopening strategy was announced (COVID19.CA.GOV, 2020).

California has particularly high air pollution rates; the 2020 'State of the Air' report from the American Lung Association ranks five California cities as having the worst air pollution from particulate matter in the nation (American Lung Association, 2020). This pollution is due, in large part to debris from wildfires (driven by climate change, Westerling and Bryant, 2008). The report also highlights extremely high ozone pollution, or smog, with six California cities demonstrating the worst levels in the nation (American Lung Association, 2020).

Based on the relatively difficult situations on both COVID-19 pandemic and air pollution in CA, the analysis between these two factors are necessary and urgent in the state.

2.2. Data

2.2.1. Ground-based air pollution observations

The ground-based observations of air pollutants are provided by the U.S. Environmental Protection Agency (EPA, https://www.epa.gov/outdoor-air-quality-data/download-daily-data). Due to data availability issues, all the accessible daily maximum 1-h concentration measurements of NO_2, daily maximum 8-h concentration of O_3, daily maximum 8-h concentration of CO, daily mean concentrations of $PM_{2.5}$ and PM_{10} are analyzed beginning on January 26, when the first confirmed case was reported in CA in 2020, and over the same period from 2015 to 2019. The data availability of each air pollutant over the study period is shown in Fig. 2.

Air pollution has crucial influences on both nature and human health (Landrigan, 2017). Different air pollutants have different emission sources, characteristics and spreading behaviors. For example, $PM_{2.5}$ describes fine inhalable particles with diameters that are generally 2.5 μm and smaller (EPA, 2019). Some $PM_{2.5}$ can be directly emitted from various sources including power plants, motor vehicles, airplanes, residential wood burning, forest fires, agricultural burning, volcanic eruptions and dust storms, while others are formed when gases and particles interact with one another in the atmosphere (Jeong et al., 2019). Therefore, other air pollutants such as sulphur dioxide and nitrogen oxides can influence the concentration of $PM_{2.5}$ (Manousakas et al., 2017). CO is a colorless, odorless, tasteless, and toxic air pollutant that is produced in the incomplete combustion of carbon-containing fuels, such as gasoline, natural gas, oil, coal, and wood (The National Academies Press, 2002). The largest anthropogenic source of CO in the United States is vehicle emissions. Indoor fuel-burning appliances such as clothes dryers, water heaters, furnaces or boilers, fireplaces (both gas and wood burning), gas stoves and ovens, motor vehicles, grills, generators, power tools, lawn equipment, wood stoves and tobacco smoke are also emission sources of CO (Wu et al., 2019). NO_2 is the greatest concerned component of nitrogen oxide, which comes from fossil-burning sources such as vehicles, power plants, industrial emissions and off-road sources such as construction, lawn and gardening equipment (EPA, 2011).

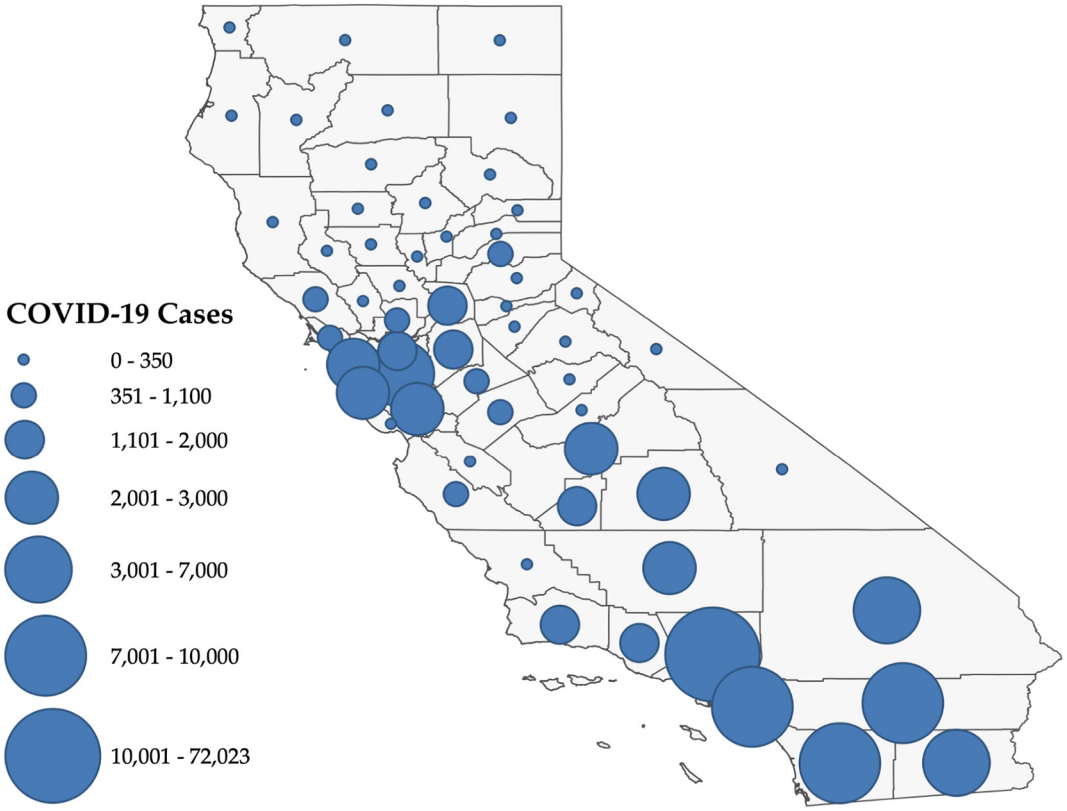

Fig. 1. Number of cumulative confirmed cases for each county in CA.

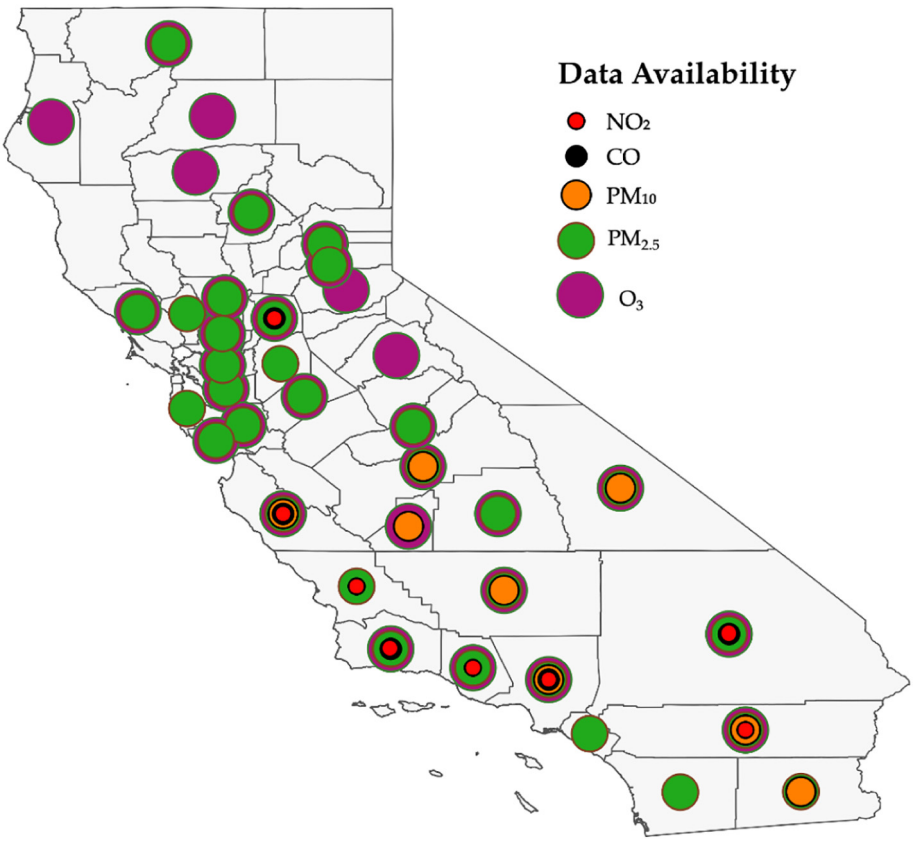

Fig. 2. Ground-based air pollution data availability for each county of California.

2.2.2. Satellite NO_2 observations

We use the Nitrogen Dioxide Product (OMNO2d) of the Ozone Monitoring Instrument (OMI) aboard NASA's Earth Observing System's (EOS) Aura satellite to calculate the mean NO_2 tropospheric vertical column density (TVCD) in the pre, *peri* and post periods of CA for both 2020 and 2015–2019. It is a level-3 gridded product where pixel-level data of good quality are binned and averaged into 0.25-degree global grids at a daily temporal resolution (Krotkov et al., 2019). OMI data is adopted to analyze the spatial patterns of COVID-19 impact on NO_2 emission.

2.2.3. Ancillary information

The paper adopts locations of major power plants, national highways and wildfires to address the potential causes on the spatial patterns of air-pollution emission in CA.

The Locations of Major Power Plants are derived from Wikipedia: List of Power Stations in California (https://en.wikipedia.org/wiki/List_of_power_stations_in_California). Information on different kinds of power stations is provided, including their locations and capacities. Natural gas and coal stations with capacity larger than 500 Megawatt are utilized in the study because NO_2 is mainly emitted from the combustion of fossil fuels such as coal and natural gas (Paraschiv and Paraschiv, 2019).

Locations of major wildfires in California during the post-period are compiled from the official website of California Department of Forestry and Fire Protection (CAL FIRE, https://www.fire.ca.gov/incidents/2020/). Fires with more than 100 acres burned are used in this study.

The Topologically Integrated Geographic Encoding and Referencing (TIGER)/Line shapefiles and related database files of national highways in California are downloaded from the official website of US Census Bureau, Department of Commerce (https://catalog.data.gov/dataset/tiger-line-shapefile-2016-nation-u-s-primary-roads-national-shapefile), which are extracted from selected geographic and cartographic information of the U.S. Census Bureau's Master Address File (MAF)/TIGER Database (MTDB, US Census Bureau, 2016).

2.3. Analytical method

The analysis was carried out by comparing the patterns and changes of air pollutants between 2020 and 2015–2019 averages as well as among pre-, peri- and post- periods in both spatial and temporal dimensions. Time series analysis is conducted using ground-based observations in the following steps:

1). For each pollutant, daily mean (or 1-h and 8-h maximum) concentrations of CA are calculated by averaging all available data during 2020 and 2015–2019 using Eq. (1):

$$C_t = \frac{\sum_{i=1}^{n} C_{i,t}}{n}, t = Jan.26, Jan.27 \ldots Jun.14 \quad (1)$$

where t is the date, C_t is the daily mean concentration of the air pollutant on date t, n is the number of available observations on this air pollutant in CA. In 2020, all the observations (of each air pollutant) in CA are averaged for each day throughout the study period. For 2015–2019, all the available measurements (of each air pollutant) in a specific date are averaged. Take January 26 as an example, the observations (of each air pollutant) on January 26 of 2015, January 26 of 2016, January 26 of 2017, January 26 of 2018 and January 26 of 2019 are averaged as the daily mean value of January 26 in 2015–2019. So as for all other dates.

2). The values achieved from step 1 are normalized to the mean of their corresponding pre period to make the two period (2020 and 2015–2019) comparable using Eq. (2):

$$NC_t = \frac{C_t}{C_{pre}} \quad (2)$$

where NC_t is the normalized daily concentration of each air pollutant, C_{pre} is the mean values of pre-periods in 2020 and 2015–2019 and is calculated based on Eq. (3):

$$C_{pre} = \frac{\sum_{t=Jan.26}^{Mar.18} C_t}{n_{pre}} \quad (3)$$

where n_{pre} is the number of days in the pre-period of 2020 and 2015–2019.

3). Time-series of 7-day moving average and standard error for each air pollutant are then calculated to smooth out daily fluctuations in air pollution monitoring.

4). The percentage change between different periods (pre-, peri- and post-periods) in 2020 and 2015–2019 are calculated respectively using Eq. (4):

$$P = \frac{C_2 - C_1}{C_1} \times 100\% \quad (4)$$

where P is percentage change between different periods, C_1 is the mean concentration of former period, C_2 is the average of latter period.

We further explore the spatial patterns of NO_2 TVCD over CA using OMI data as follows:

a. The average NO_2 TVCD in pre-, peri- and post- periods of 2020 and 2015–2019 are calculated for each pixel within CA based on Eq. (5):

$$\mathrm{TVCD}_i = \frac{\sum_{t=start\ date}^{end\ date} \mathrm{TVCD}_{i,t}}{n} \quad (5)$$

where TVCD_i is the average NO_2 TVCD of the ith pixel in each period; start date and end date correspond to the first and last date of each period; n is the number of days in the period. More specifically, the annual mean values of each pixel in each period of 2020 and 2015–2019 are calculated by averaging all the daily values in this period in 2020 and 2015–2019 respectively.

b. To rule out the possible influence of seasonal variations on NO_2 TVCD, we calculate the anomalies by subtracting the annual mean values of 2015–2019 from 2020 for each period;

c. Differences between peri- and pre-, post- and pre-, and post- and peri-period are calculated based on anomalies achieved in step (b).

d. Locations of major power plants, national highways and wildfires are utilized to explain the derived patterns.

3. Results

3.1. Time series analysis

As shown in Fig. 3, the concentrations of air pollutants are normalized to the means of the pre-period. Note that the NO_2 and CO data in 2020 are generally lower than in previous years without normalization, probably reflecting in part the effects of clean power plans to limit air pollution emissions from future and existing fossil-fueled power plants (Burtraw et al., 2015) and, more widely, the popularization of zero-emission vehicles in CA (McConnell et al., 2019).

At the beginning of March (2020), all pollutants demonstrate a drastic drop compared to the relatively stable curve of previous year and hold steady at a period of low values thereafter. This can be attributed to the state of emergency declared on March 4, after the first death in CA attributable to coronavirus occurred in Placer County. By the end of April, concentrations of O_3, $PM_{2.5}$ and PM_{10} returned to a normal trend (compared to the 2015–2019 period) which may be correlated to the gradual resumption of economic activities. O_3 and $PM_{2.5}$ maintain a similar pattern with historical data thereafter, however, PM_{10} keeps increasing at a higher rate after bouncing back to the level of the pre-

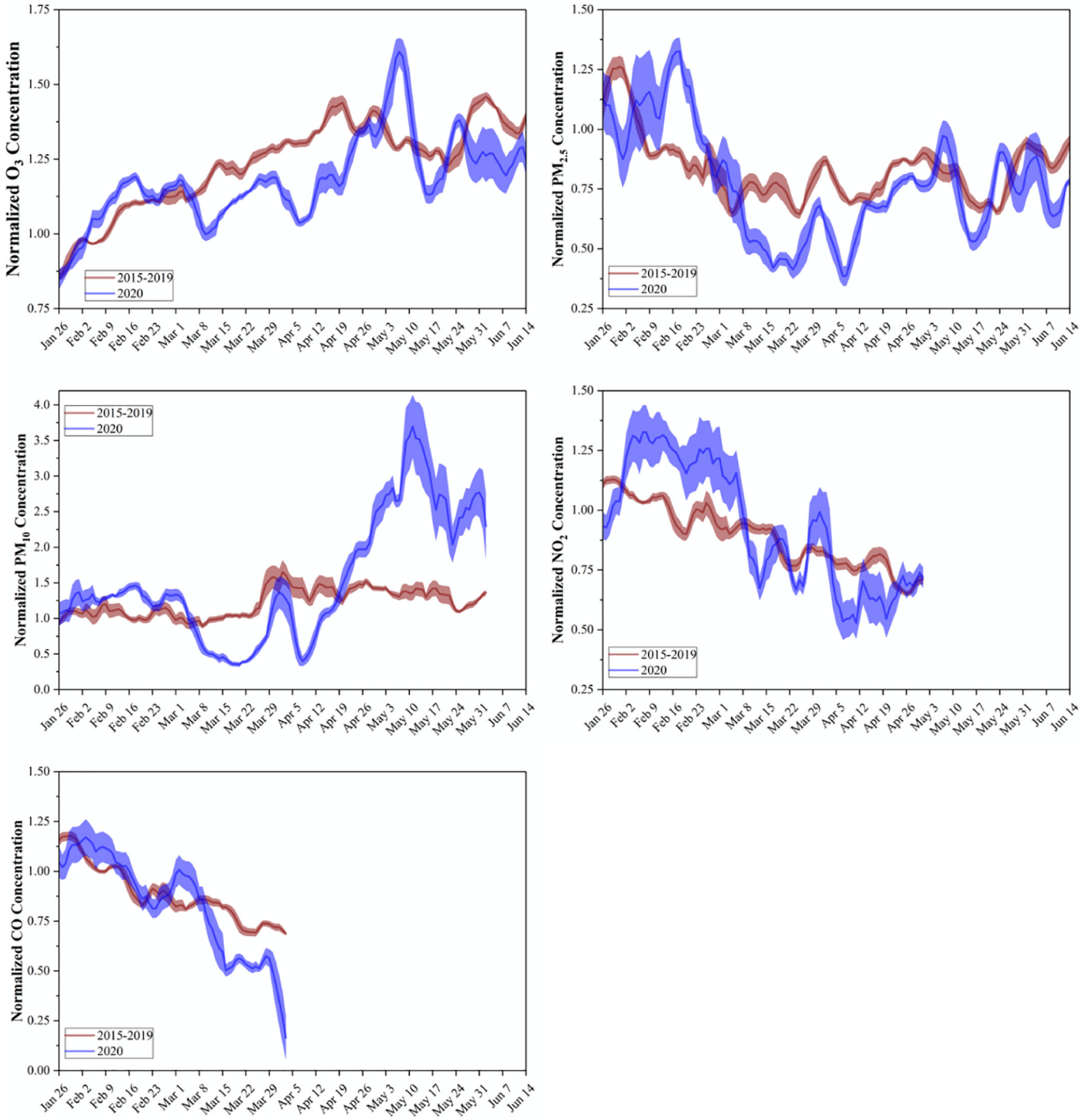

Fig. 3. Daily variations in 7-day moving averages of the concentration for each pollutant over CA. Dates represent the midpoint of the 7-day interval. Values are normalized to the mean of the pre-*peri*od. The shadows represent standard errors. The missing periods of PM_{10}, NO_2 and CO are due to the lack of data.

period. This pattern can be attributed to the increasing number of wildfires around CA since the beginning of May (https://www.fire.ca.gov/incidents/2020/), for debris produced by wildfires are one of the major sources of PM_{10} (Caseiro et al., 2009).

Ground-based observations show a 38%, 49%, and 31% drop in the concentration of NO_2, CO and $PM_{2.5}$ during *peri*-period compared to pre-period in 2020. These are 16%, 25%, and 19% sharper than in the means of the same periods in 2015–2019, respectively. Meanwhile, 21% and 14% increases are found in PM_{10} and O_3, which are 11% and 10% lower than in previous five years. After the reopening of California, $PM_{2.5}$, PM_{10} and O_3 increase by 17%, 114% and 4% compared to 3%, −5% (decrease) and 0.9% in 2015–2019. Therefore, policy interventions to reduce the spread of COVID-19 in CA such as lockdowns and reopening have clear influences on the temporal pattern of air pollution. The lockdown intensified the decreasing trends and impeded increasing trends of pollutants, while the reopening brought the trends back on track compared to previous years.

There is a 51% drop in CO concentration during the *peri*-period of 2020 compared to the same period of 2015–2019, which is more significant than that of NO_2 and $PM_{2.5}$ (46% and 25% respectively). As

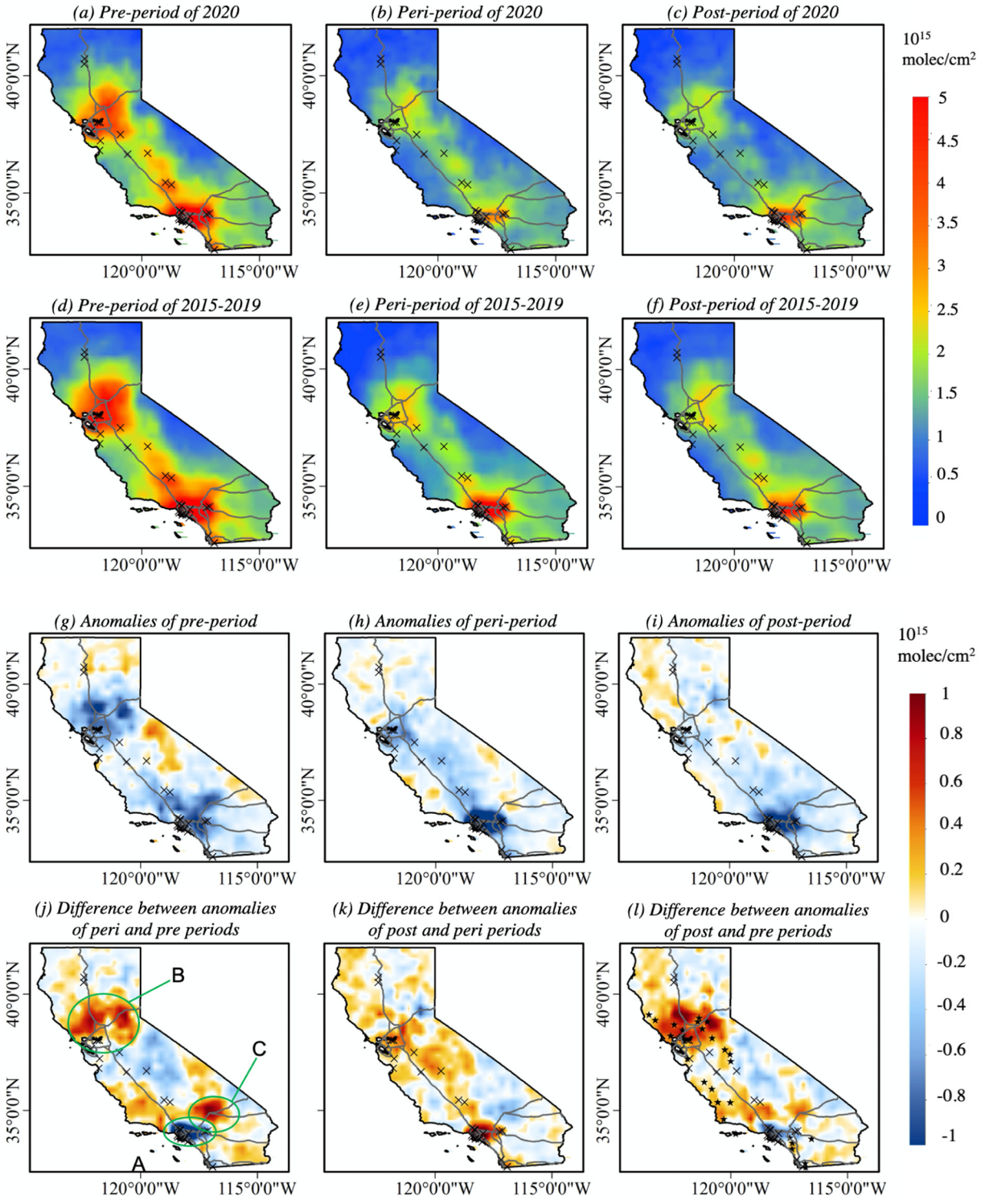

Fig. 4. Spatial patterns of tropospheric NO_2 TVCD over CA. (a)–(f) are average OMI tropospheric NO_2 vertical column densities in 2020 and previous years: (a) pre-period in 2020, (b) peri-period in 2020, (c) post-period in 2020, (d) pre-period in 2015–2019, (e) peri-period in 2015–2019, and (f) post-period in 2015–2019. (g)–(i) are anomalies of pre, peri and post periods: (g) anomalies of pre-period; (h) anomalies of peri-period; (i) anomalies of post-period. (j)–(l) are differences among pre, peri and post periods: (j) difference between anomalies of peri and pre periods; (k) difference between anomalies of post and peri periods; and (l) difference between anomalies of post and pre periods. The ×s are locations of major power plants in CA. The stars are locations of wildfires occurred in the post- period and the grey lines show U.S. National Highways.

previously illustrated, statistical results also show a sharper decline in CO concentration than NO_2 and $PM_{2.5}$ when comparing between peri-period and pre-period in 2020 (49% vs 38% and 31%). Therefore, CO has a larger decrease than the other two air pollutants. And the concentration of $PM_{2.5}$ has the gentlest decline in these three air pollutants.

3.2. Spatial pattern analysis

Fig. 4 shows spatial patterns of NO_2 TVCD over CA in 2020 and 2015–2019. As shown in Fig. 4(a)–(c), TVCD of NO_2 is generally lower in the peri period than pre and rebounds over some regions in the post

period. The overall NO_2 emissions decrease by 33% and 0.6% in the peri and post-period respectively than the pre-period, compared to 30% and 3% in 2015–2019. Although the statistics are not exactly the same as ground-based observations, the sudden drop following the lockdown order is also captured by satellite data. Fig. 4(g)–(i) are the anomalies of pre, peri and post periods respectively. Most regions of CA show negative values in all three periods, demonstrating that the mean value of 2020 is generally lower than 2015–2019. This can also be observed in EPA data due to the air quality protection policies mentioned in previous sections.

As shown in Fig. 4(j), the anomalies of NO_2 TVCD decrease significantly in the peri- period compared to the pre- period over region A and rebound in the post- period according to Fig. 4 (k). Still, this uptick is not large enough to remedy the lockdown reductions, which can be observed in Fig. 4(l). There are many power plants concentrated around region A; NO_2 TVCD is dominated by emissions from power plants in this area. Due to the scale-back of non-essential industries in response to COVID-19 crisis, NO_2 declines in region A during the lockdown and recovers partially after reopening when they gradually go back to work. California Independent System Operator (CAISO) reported a 6.7% reduction of energy loads in peak hours of weekdays during the lockdown. Higher loads were observed by the end of May during the implementation of gradual reopening policies (CAISO, 2020).

Over regions B and C, NO_2 anomalies increase dramatically in the peri- period (Fig. 4(j)) and then drop in the post- period (Fig. 4(k)). The entirety of region C and some of region B show negative values in the comparison between post- and peri- period, however, the post-period is still higher than the pre- period, as can be observed in Fig. 4(l).

On one hand, fuel-burning from everyday domestic activities are an important source of NO_2 emissions in residential areas (Lee et al., 2002), such as heaters and stoves (Kousa et al., 2001). Both B and C are populous regions and transportation hubs that are located at intersections of national highways including the city of Barstow, Napa and Woodland. It can be intuited that citizens spent more time staying in residential areas during the peri- period due to the stay-at-home orders and social distancing policies and would likely produce more NO_2 in their daily lives.

On the other hand, transportation (which produces large amounts of NO_2) between different cities is reduced, which indicates decreasing NO_2 emissions along many parts of the national highways. Still, essential vehicular use likely increased within residential areas—especially those serving as transportation hubs—such as greater utilization of food and grocery deliveries (Sarmiento, 2020) and cargo transportation (Bates, 2020). After stepping into the post- period, people started to resume their normal lives and residential NO_2 levels drop compared with peri- period; levels are still higher than pre- period in region C due to the incompleteness of reopening. Region C is primarily located within the Mojave Desert Air Basin. Prevailing winds are understood to channel air masses through this basin due to the close proximity to the coast and mountain ranges alongside the strong influence of Santa Ana winds (VanCuren and Gustin, 2015). With a likely increase in transportation during the lockdown within city limits and Santa Ana winds ending in March, this combination of factors can impact NO_2 fluctuations in the transportation hub (SB County, 2020).

Furthermore, more wildfires occurred in region B in the post-period resulting in a higher discharge of NO_2 (Martin et al., 2006) than the pre- period (Fig. 4(l)). Therefore, we do not observe a simple declining pattern in region C in Fig. 4(k). Similar trends can be found in other residential and wildfire locations.

Note that the increase/decrease of NO_2 anomalies over one region does not mean a higher/lower absolute TVCD value; it indicates more/less NO_2 is emitted due to non-seasonal factors. NO_2 primarily pollutes the air from the burning of fossil fuel such as emissions from cars, trucks and buses, power plants, and off-road equipment. Given that most non-essential businesses are shutdown or limited in peri- and post- periods, COVID-19 related shutdown and reopening policies are the most likely reasons accounting for the change of NO_2 spatial patterns, especially when there are no major wildfires.

4. Discussion

To combat the spread of COVID-19 pandemic, the CA government implemented a series of policies including the shutdown of non-essential businesses, mandating social distancing, and the prohibition of large gatherings. These measures caused non-negligible influences on the air pollution emissions which reflect statewide economic conditions. This paper analyzed the spatiotemporal patterns and changes of air pollution before, during and after the lockdown of CA since the first confirmed COVID-19 case was reported in the state. The concentrations of air pollution are influenced by complex variables such as wind, temperature, burning material, policies and other anthropogenic factors. This study accounts for the seasonal-cycle related impacts by comparing the 2020 data with the means of the previous five years. Then potential effects of COVID-19 are further explored by combining the analysis with the locations of major power plants, wildfires and national highways in California.

Through time series analysis, we find that when interventional policies are implemented to mitigate the COVID-19 crisis, the temporal trends of air pollutants present correspondence to the policy order dates. Once the shutdown and stay-at-home policies were implemented, the time series data show significant pollution reductions; when the reopening phases are put into effect, pollution rebounds to normal trends, as compared with previous years.

Spatial patterns of tropospheric NO_2 TVCD are also influenced by COVID-19 policy interventions. Decreases are observed around the locations of power plants while increases occurred in residential regions following the lockdown order. Ruling out the seasonal trends and natural factors such as wildfires, the restriction of non-essential industries and quarantine of people in residential areas are the most likely factor to account for these patterns. Although transportation was reduced between cities, it increased within residential communities, especially those serving as transportation hubs.

Although overall trends are similar in ground-based observations and satellite data, discrepancies still exist between the two data sources mainly due to the following reasons:

(1) Ground stations monitor the concentrations of air pollutants near the surface, whereas satellite data retrieves the vertical column density of NO_2 in troposphere;
(2) Ground-based observations are sparsely distributed; not every county in CA has available data.
(3) Ground-based NO_2 data reflects daily mean 1-h maximum concentrations while satellite observations are retrieved at the moment when the sensor scanned across the area.

This study is an initial effort to understand the impact of COVID-19 mitigation efforts on air pollution and several related factors still have not been quantitatively considered. For example, the patterns of air pollution could also be influenced by climate and geographical changes, such as global warming (Williams et al., 2019) and vegetation (Solins et al., 2018). Although these effects are partially accounted for by comparing with previous years and observing anomalies, they cannot be entirely eliminated from the results, leading to complex interaction of influential variables in some regions. Spontaneous reduction in human mobility before the lockdown announcement could also influence air pollution emissions (Chinazzi et al., 2020), especially those relating to inter-state and international travels. Detailed transportation volumes within residential areas also need to be further investigated and integrated into a comprehensive analysis.

Similar studies have been done by other researchers in other areas or scales. Liu et al. (2020a, 2020b) conducted a similar study in China and found that satellite measurements showed a 48% drop in NO_2 TVCD from the 20 days averaged before the lockdown to the 20 days averaged after. This decline is 21% larger than that from 2015 to 2019. The drop from the pre- to peri-period in California was 33% in 2020, which is 3%

larger than that of 2015–2019. Compared to China, California has a relatively smaller decline and variation in NO_2 TVCD due to the COVID-19 mitigation policies. Berman and Ebisu (2020) assessed air quality during the COVID-19 pandemic NO_2 in the continental United States and discovered a 26% and a 5% reduction in NO_2 and $PM_{2.5}$ respectively in 2020 compared to the same period in 2017–2019. The declines are 46% and 25% for NO_2 and $PM_{2.5}$ respectively during peri-periods between 2020 and previous years. The drops in air pollutants are more significant in California than the US overall may be potentially due to the fact that air pollution before the pandemic is more severe (American Lung Association, 2020) and mitigation-policy stringency in CA is higher than most of other states (12 out of 54, Fig. A.2). The European Environment Agency detected a similar large drop in air pollution across European cities (European Environmental Agency, 2020). From March 16 to 22, 2020, it was reported that Bergamo, Italy and Barcelona, Spain showed declines of 47% and 55% in NO_2 compared to the same period in 2019. These numbers are comparable to that of California (46%) in the peri-period.

Despite the effort made by this study and all the other research, more work needs to be done on the impact of COVID-19 mitigation efforts, including:

(1) Conducting similar research over other parts of the world especially those areas that have rarely been studied, such as Africa, and analyzing the impact of COVID-19 mitigation efforts on different income groups, e.g. low-income countries and high-income countries.
(2) Including other potential factors that affect the patterns and trend of air pollution such as human mobilities, inner-city transportation, climate and geographical changes, to isolate the influence of COVID-19 mitigation efforts more accurately;
(3) Further investigation of the COVID-19 impacts after reopening is carried out.
(4) Investigating the impact of COVID-19 mitigation efforts on the California economy.
(5) Studying the impact of air pollution and other climate factors on the spread of COVID-19.

5. Conclusions

According to the experiments and analysis results, this study has come to the following conclusions:

(1) The spatiotemporal patterns of air pollution in CA were influenced by the COVID-19 mitigation lockdown and reopening policies.
(2) The lockdown policy generally reduced the concentration of air pollutants in CA; the reopening increased the emissions of air pollution back to a normal trend, as compared to previous years.
(3) The concentration of CO has a sharper decline than that of NO_2 and $PM_{2.5}$ during the pandemic.
(4) NO_2 emissions decreased over locations of major power plants and increased over populous residential areas, especially those serving as transportation hubs at the intersections of national highways.

CRediT authorship contribution statement

Qian Liu: Conceptualization, Investigation, Visualization, Writing - original draft. **Jackson T. Harris:** Investigation, Visualization, Writing - review & editing. **Long S. Chiu:** Conceptualization, Supervision. **Donglian Sun:** Conceptualization, Writing - review & editing. **Paul R. Houser:** Conceptualization, Writing - review & editing. **Manzhu Yu:** Writing - review & editing. **Daniel Q. Duffy:** Conceptualization, Funding acquisition. **Michael M. Little:** Funding acquisition, Resources. **Chaowei Yang:** Conceptualization, Supervision, Writing - review & editing, Funding acquisition.

Declaration of competing interest

The authors declare that they have no known competing financial interests or personal relationships that could have appeared to influence the work reported in this paper.

Acknowledgements

The study is funded by NSF I/UCRC program and Covid-19 rapid response program and NASA Center for Climate Simulations; ground-based air pollution data were downloaded from EPA website: https://www.epa.gov/outdoor-air-quality-data/download-daily-data; OMI NO_2 data are from GES DISC: https://disc.gsfc.nasa.gov/datasets/OMNO2d_003/summary?keywords=omi; locations of major power plants in CA are achieved from Wikipedia: https://en.wikipedia.org/wiki/List_of_power_stations_in_California; locations of major wildfires are downloaded from California Department of Forestry and Fire Protection (CAL FIRE): https://www.fire.ca.gov/incidents/2020/; the locations of national highways in California are obtained from the official website of US Census Bureau, Department of Commerce: https://catalog.data.gov/dataset/tiger-line-shapefile-2016-nation-u-s-primary-roads-national-shapefile.

Appendix A. Supplementary data

Supplementary data to this article can be found online at https://doi.org/10.1016/j.scitotenv.2020.141592.

References

American Lung Association, 2020. State of the air. Available at: http://www.stateoftheair.org/assets/SOTA-2020.pdf (2020) Accessed date: June 21 2020.
Bao, R., Zhang, A., 2020. Does lockdown reduce air pollution? Evidence from 44 cities in northern China. Sci. Total Environ. 731, 139052.
Bates, J., 2020. Cargo volumes soar at Ontario International Airport. https://airport-world.com/cargo-volumes-soar-at-ontario-international-airport/ Accessed date: June 5 2020.
Berman, J.D., Ebisu, K., 2020. Changes in US air pollution during the COVID-19 pandemic. Sci. Total Environ. 739, 139864.
Burtraw, D., Bushnell, J., Munnings, C., 2015. State and Regional Comprehensive Carbon Pricing and Greenhouse Gas Regulation in the Power Sector Under EPA's Clean Power Plan: Workshop Summary. Resources for the Future Discussion Paper. pp. 15–31.
CAISO. COVID-19 Impacts to California ISO Load & Markets: March 17–June 7, 2020. Available at: http://www.caiso.com/Documents/COVID-19-Impacts-ISOLoadForecast-Presentation.pdf (2020) Accessed date: June 22 2020.
Caseiro, A., Bauer, H., Schmidl, C., Pio, C.A., Puxbaum, H., 2009. Wood burning impact on PM_{10} in three Austrian regions. Atmos. Environ. 43 (13), 2186–2195.
Chinazzi, M., Davis, J.T., Ajelli, M., Gioannini, C., Litvinova, M., Merler, S., y Piontti, A.P., Mu, K., Rossi, L., Sun, K. and Viboud, C., 2020. The effect of travel restrictions on the spread of the 2019 novel coronavirus (COVID-19) outbreak. Science, 368(6489), pp.395–400.
COVID19.CA.GOV, 2020. Resilience Roadmap.Available at. https://covid19.ca.gov/roadmap/#top Accessed date: June 22 2020.
Dutheil, F., Baker, J.S., Navel, V., 2020. COVID-19 as a factor influencing air pollution? Environmental Pollution (Barking, Essex: 1987) 263, 114466.
EPA, 2011. Air quality guide for nitrogen dioxide. https://www3.epa.gov/airnow/no2.pdf Access on July 25 2020.
EPA, 2019. Particulate matter ($PM_{2.5}$) trends. https://www.epa.gov/air-trends/particulate-matter-pm25-trends Access on July 25 2020.
European Environment Agency, 2020. https://www.eea.europa.eu/highlights/air-pollution-goes-down-as Accessed 26 July 2020.
Hilboll, A., Richter, A., Burrows, J.P., 2017. NO_2 pollution over India observed from space–the impact of rapid economic growth, and a recent decline. Atmos. Chem. Phys. Discuss 20, 1–18.
Jeong, C.H., Wang, J.M., Hilker, N., Debosz, J., Sofowote, U., Su, Y., Noble, M., Healy, R.M., Munoz, T., Dabek-Zlotorzynska, E., Celo, V., 2019. Temporal and spatial variability of traffic-related $PM_{2.5}$ sources: comparison of exhaust and non-exhaust emissions. Atmos. Environ. 198, 55–69.
Kousa, A., Monn, C., Rotko, T., Alm, S., Oglesby, L., Jantunen, M.J., 2001. Personal exposures to NO_2 in the EXPOLIS-study: relation to residential indoor, outdoor and workplace concentrations in Basel, Helsinki and Prague. Atmos. Environ. 35 (20), 3405–3412.
Nickolay A. Krotkov, Lok N. Lamsal, Sergey V. Marchenko, Edward A. Celarier, Eric J. Bucsela, William H. Swartz, Joanna Joiner and the OMI core team (2019), OMI/Aura NO2 Cloud-Screened Total and Tropospheric Column L3 Global Gridded 0.25 Degree × 0.25 Degree V3, NASA Goddard Space Flight Center, Goddard Earth Sciences Data and Information Services Center (GES DISC), Accessed at: 10.5067/Aura/OMI/DATA3007 (2020) Accessed date: June 22 2020.

Landrigan, P.J., 2017. Air pollution and health. Lancet Public Health 2 (1), e4–e5.
Lee, K., Xue, J., Geyh, A.S., Ozkaynak, H., Leaderer, B.P., Weschler, C.J., Spengler, J.D., 2002. Nitrous acid, nitrogen dioxide, and ozone concentrations in residential environments. Environ. Health Perspect. 110 (2), 145–150.
Liu, F., Page, A., Strode, S.A., Yoshida, Y., Choi, S., Zheng, B., Lamsal, L.N., Li, C., Krotkov, N.A., Eskes, H., Veefkind, P., 2020a. Abrupt decline in tropospheric nitrogen dioxide over China after the outbreak of COVID-19. Sci. Adv. eabc2992.
Liu, Q., Sha, D., Liu, W., Houser, P., Zhang, L., Hou, R., Lan, H., Flynn, C., Lu, M., Hu, T., Yang, C., 2020b. Spatiotemporal patterns of COVID-19 impact on human activities and environment in mainland China using nighttime light and air quality data. Remote Sens. 12 (10), 1576.
Manousakas, M., Papaefthymiou, H., Diapouli, E., Migliori, A., Karydas, A.G., Bogdanovic-Radovic, I., Eleftheriadis, K., 2017. Assessment of $PM_{2.5}$ sources and their corresponding level of uncertainty in a coastal urban area using EPA PMF 5.0 enhanced diagnostics. Sci. Total Environ. 574, 155–164.
Martin, M.V., Honrath, R.E., Owen, R.C., Pfister, G., Fialho, P., Barata, F., 2006. Significant enhancements of nitrogen oxides, black carbon, and ozone in the North Atlantic lower free troposphere resulting from North American boreal wildfires. Journal of Geophysical Research: Atmospheres 111 (D23).
McConnell, V., Leard, B., Kardos, F., 2019. California's Evolving Zero Emission Vehicle Program: Pulling New Technology into the Market. Working Paper. Washington, DC: Resources for the Future.
Muhammad, S., Long, X., Salman, M., 2020. COVID-19 pandemic and environmental pollution: a blessing in disguise. Sci. Total Environ. 138820.
NSF Spatiotemporal Innovation Center, 2020. COVID-19 spatiotemporal rapid response gateway. Accessed at. https://covid-19.stcenter.net/index.php/covid19-livemap/ Accessed date: June 14 2020.
Paraschiv, S., Paraschiv, L.S., 2019. Analysis of traffic and industrial source contributions to ambient air pollution with nitrogen dioxide in two urban areas in Romania. Energy Procedia 157, 1553–1560.
Raifman, J., Nocka, K., Jones, D., Bor, J., Lipson, S., Jay, J., Chan, P., Galea, S., 2020. COVID-19 US State Policy Database. Inter-university Consortium for Political and Social Research [distributor], Ann Arbor, MI 2020-06-04. https://doi.org/10.3886/E119446V1.
Russell, A.R., Valin, L.C., Cohen, R.C., 2012. Trends in OMI NO_2 observations over the United States: effects of emission control technology and the economic recession. Atmos. Chem. Phys. 12 (24), 12197.
Saadat, S., Rawtani, D., Hussain, C.M., 2020. Environmental perspective of COVID-19. Sci. Total Environ. 138870.
San Bernardino County, 2020. County wire. Accessed at. https://wp.sbcounty.gov/cao/countywire/ Accessed date: June 22 2020.
Sarmiento, I.G., 2020. As restaurants across the country close their doors, deliveries pick up. Accessed at. https://www.npr.org/2020/03/22/819011691/as-restaurants-across-the-country-close-their-doors-deliveries-pick-up Accessed date: June 22 2020.
Sinha, A., 2016. Trilateral association between SO_2/NO_2 emission, inequality in energy intensity, and economic growth: a case of Indian cities. Atmospheric pollution research 7 (4), 647–658.
Solins, J.P., Thorne, J.H., Cadenasso, M.L., 2018. Riparian canopy expansion in an urban landscape: multiple drivers of vegetation change along headwater streams near Sacramento, California. Landsc. Urban Plan. 172, 37–46.
The National Academies Press, 2002. The Ongoing Challenge of Managing Carbon Monoxide Pollution in Fairbanks, Alaska: Interim Report. https://www.nap.edu/read/10378/chapter/3 Access on July 25 2020.
US Census Bureau, 2016. TIGER/Line Shapefile, 2016, Nation, U.S., Primary Roads National Shapefile. Accessed at. https://catalog.data.gov/dataset/tiger-line-shapefile-2016-nation-u-s-primary-roads-national-shapefile 2016. Accessed date: June 10 2020.
VanCuren, R.T., Gustin, M.S., 2015. Identification of sources contributing to PM2. 5 and ozone at elevated sites in the western US by receptor analysis: Lassen volcanic National Park, California, and Great Basin National Park, Nevada. Sci. Total Environ. 530, 505–518.
Wang, Y., Zhuang, G., Zhang, X., Huang, K., Xu, C., Tang, A., Chen, J., An, Z., 2006. The ion chemistry, seasonal cycle, and sources of $PM_{2.5}$ and TSP aerosol in Shanghai. Atmos. Environ. 40 (16), 2935–2952.
Wang, P., Chen, K., Zhu, S., Wang, P., Zhang, H., 2020. Severe air pollution events not avoided by reduced anthropogenic activities during COVID-19 outbreak. Resour. Conserv. Recycl. 158, 104814.
Westerling, A.L., Bryant, B.P., 2008. Climate change and wildfire in California. Clim. Chang. 87 (1), 231–249.
Williams, A.P., Abatzoglou, J.T., Gershunov, A., Guzman-Morales, J., Bishop, D.A., Balch, J.K., Lettenmaier, D.P., 2019. Observed impacts of anthropogenic climate change on wildfire in California. Earth's Future 7 (8), 892–910.
Wu, Y., Zhang, Y., Zhou, C., Wang, J., Wu, J., Ren, T., 2019. Study of CO sources and early-warning concentration of spontaneous combustion at air return corner in fully mechanized mining faces. Combust. Sci. Technol. 1–18.
Wu, X., Nethery, R.C., Sabath, B.M., Braun, D., Dominici, F., 2020. Exposure to air pollution and COVID-19 mortality in the United States. medRxiv.
Yang, C., Yu, M., Li, Y., Hu, F., Jiang, Y., Liu, Q., Sha, D., Xu, M., Gu, J., 2019. Big Earth data analytics: a survey. Big Earth Data 3 (2), 83–107.
Yang, C., Sha, D., Liu, Q., Li, Y., Lan, H., Guan, W.W., Hu, T., Li, Z., Zhang, Z., Thompson, J.H., Wang, Z., Wong, W., Ruan, S., Yu, M., Richardson, D., Zhang, L., Hou, R., Zhou, Y., Zhong, C., Tian, Y., Beaini, F., Carte, K., Flynn, C., Liu, W., Pfoser, D., Bao, S., Li, M., Zhang, H., Liu, C., Jiang, J., Du, S., Zhao, L., Lu, M., Li, L., Zhou, H., 2020. Taking the pulse of COVID-19: a spatiotemporal perspective. arXiv preprint. (arXiv: 2005.04224v1).
Yang, C., Clarke, K., Shekhar, S., Tao, C.V., 2020b. Big spatiotemporal data analytics: a research and innovation frontier. Int. J. Geogr. Inf. Sci. 34 (6), 1075–1088.
Zhang, Z., Xue, T., Jin, X., 2020. Effects of meteorological conditions and air pollution on COVID-19 transmission: evidence from 219 Chinese cities. Sci. Total Environ. 140244.
Zhu, Y., Xie, J., Huang, F., Cao, L., 2020. Association between short-term exposure to air pollution and COVID-19 infection: evidence from China. Sci. Total Environ. 138704.